NASA TECHNICAL NOTE

NASA TN D-4851

NASA TN D-4851

EFFECT OF THRUST PER ELEMENT ON COMBUSTION STABILITY CHARACTERISTICS OF HYDROGEN-OXYGEN ROCKET ENGINES

by Reino J. Salmi, John P. Wanhainen, and Ned P. Hannum

Lewis Research Center
Cleveland, Ohio

NATIONAL AERONAUTICS AND SPACE ADMINISTRATION • WASHINGTON, D. C. • OCTOBER 1968

EFFECT OF THRUST PER ELEMENT ON COMBUSTION STABILITY CHARACTERISTICS OF HYDROGEN-OXYGEN ROCKET ENGINES

By Reino J. Salmi, John P. Wanhainen, and Ned P. Hannum

Lewis Research Center
Cleveland, Ohio

NATIONAL AERONAUTICS AND SPACE ADMINISTRATION

For sale by the Clearinghouse for Federal Scientific and Technical Information
Springfield, Virginia 22151 – CFSTI price $3.00

ABSTRACT

The results obtained with a series of 10.78-inch (0.27-m) coaxial injectors on a 20 000-pound (88 964-N) thrust oxygen-hydrogen rocket engine operated at a chamber pressure of 300 psia (2.064 MN/m^2) were analyzed to determine the effects of injector thrust per element T/E on the combustion stability. The thrust per element ranged from about 20 to 2500 pounds (88.96 to 11 120 N). Based on the minimum hydrogen temperature for stable combustion, the combustion stability increased with increasing thrust per element. No combustion instability was observed at a thrust per element of 200 pounds (889.6 N) or above. Bombing of the 572 and 1000 pound (2542 and 4448 N) T/E injectors failed to induce combustion instability. The hydrogen transition temperatures of the unstable injectors showed agreement with two different correlating parameters.

EFFECT OF THRUST PER ELEMENT ON COMBUSTION STABILITY CHARACTERISTICS OF HYDROGEN-OXYGEN ROCKET ENGINES

by Reino J. Salmi, John P. Wanhainen, and Ned P. Hannum
Lewis Research Center

SUMMARY

The Lewis Research Center has conducted a program to investigate the combustion stability of hydrogen-oxygen rocket engines using a 20 000-pound (88 964-N) thrust heat-sink engine operated at a chamber pressure of 300 psia (2.064 MN/m^2). The results obtained with a series of coaxial injectors were analyzed to determine the effects on the combustion stability of injector thrust per element. The injectors varied slightly in the hydrogen-to-oxygen injection area ratio, face plate material, and thickness. All except two injectors had elements placed uniformly over the injector face. The thrust-per-element T/E ranged from about 20 to 2500 pounds (88.96 to 11 120 N).

Based on the minimum hydrogen-injection temperature for stable combustion, the combustion stability increased with increasing T/E. No instability was obtained with injectors having a T/E of 200 pounds (889.6 N) or greater. Bombing of the 572 and 1000 pound (2542 and 4448 N) injectors failed to induce combustion instability. The hydrogen transition temperatures of the unstable injectors showed agreement both for a correlating parameter obtained by multiplying the propellant injection velocity ratio by the propellant weight flow per element and for the W_{cr} parameter of reference 12.

INTRODUCTION

High-frequency combustion-chamber pressure oscillations or "screech" is a continuing problem for designers of liquid-propellant rocket engines. Although the causes of this instability are elusive, they are being illuminated by both theoretical and experimental research. Most prominent of the analytical approaches is the sensitive time-lag theory of Crocco (ref. 1). Another promising analytical approach is the engine system dynamic response model reported in reference 2.

At the Lewis Research Center, an extensive experimental research program has

been conducted to define the effects of various engine design parameters on the combustion instability phenomenon. A 20 000-pound (88 964-N) thrust hydrogen-oxygen rocket engine using coaxial element injectors was used.

From the early results of the program, some empirical relations have been formulated (such as those of ref. 3) relating rocket-engine operating and geometrical variables with the occurrence of combustion instability. The hydrogen-injection temperature at which stable combustion changed to unstable combustion was used as a convenient measure of the relative stability of various engine configurations.

In studying the results obtained from tests with injectors having various numbers of elements, it was noted that the stability appeared to be influenced by the number of elements or, since the thrust was constant, by the engine thrust per element. Although no subprogram designed to vary only thrust per element had been conducted it was considered worthwhile to analyze the existing data from the viewpoint of thrust per element.

Presented herein are results obtained with 10.78-inch (27.4-cm) diameter coaxial injectors that contained from 20 to 992 elements. The corresponding thrust-per-element varied from about 1000 to 20 pounds (4448 to 88.96 N). The injectors differed slightly in the hydrogen-to-oxygen injection area ratio and in the faceplate material and thickness. Also presented are some results from reference 4 for an eight-element 2500-pound (11 120-N) thrust per element T/E injector.

The rocket firings were conducted in a sea-level test stand with heat-sink engines. The engines developed 20 000 pounds (88 964 N) thrust at a chamber pressure of 300 psia (2.064 MN/m^2). After steady-state operation at the design chamber pressure was reached, the hydrogen temperature at which instability occurred was obtained by ramping the hydrogen temperature from an initial high value to either the minimum value obtainable with the test facility or to a temperature low enough to definitely establish combustion instability. In attempts to trigger combustion instability, tangential bomb pulses were used with the 572- and 1000-pound (2542- and 4448-N) T/E injectors. The oxidant-fuel ratio was held constant for each test at nominal values of 4, 5, and 6.

APPARATUS

Test Facility

The investigation was conducted at the Lewis Rocket Engine Test Facility. This is a 50 000-pound (222 410-N) sea-level rocket test stand equipped with an exhaust gas muffler and scrubber. The rocket engines were mounted on a thrust stand to fire vertically into the scrubber. The facility used pressurized propellant-storage tanks to pump the propellants to the rocket engine.

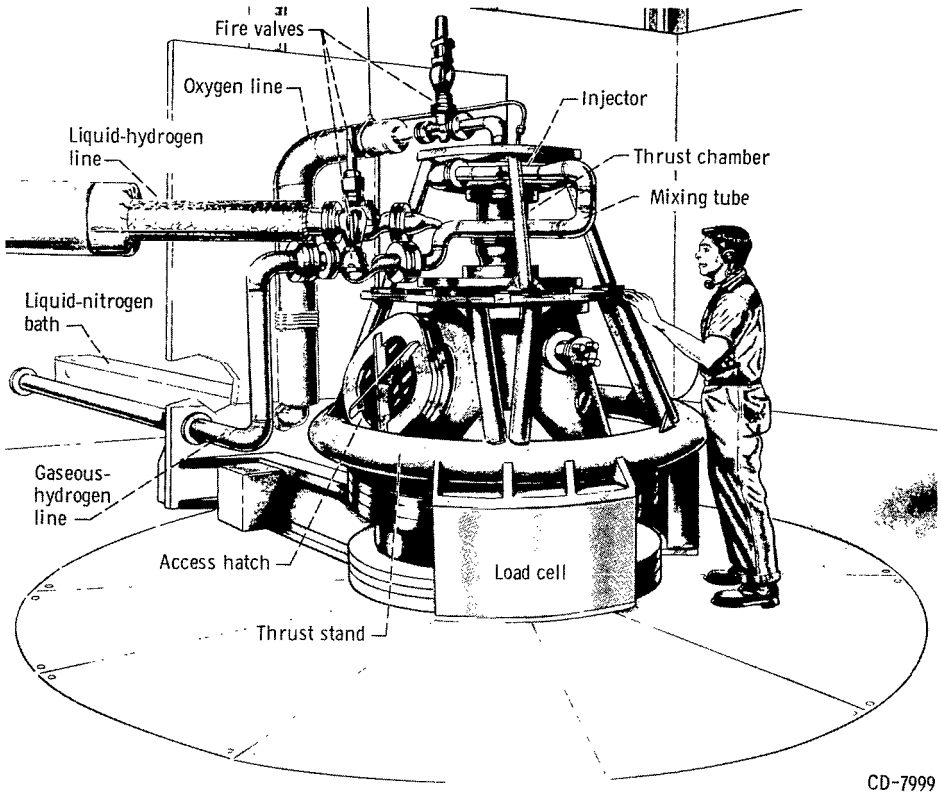

Figure 1. - Engine mounted on thrust stand.

A sketch of the engine test stand is shown in figure 1. A mixing tube to vary the temperature of the hydrogen to the engine was located in the section of line just downstream of the liquid hydrogen and gaseous hydrogen engine fire valves.

Engine

The rocket engine (fig. 2) was comprised of an injector, a cylindrical 10.78-inch (0.274-m) inside-diameter heat-sink thrust chamber 12 inches (0.305 m) long and a convergent-divergent heat-sink exhaust nozzle. The nozzle had a throat area of 47.91 square inches (0.0309 m^2) and a contraction ratio of 1.89. The expansion ratio was 1.3. The inner surfaces of the combustion chamber and exhaust nozzle were coated with 0.030 inch (0.772 mm) of flame-sprayed zirconium oxide to reduce the heat transfer to the metal. The thrust chambers could be operated for 3 seconds without damage. This run duration was adequate to obtain the desired test results.

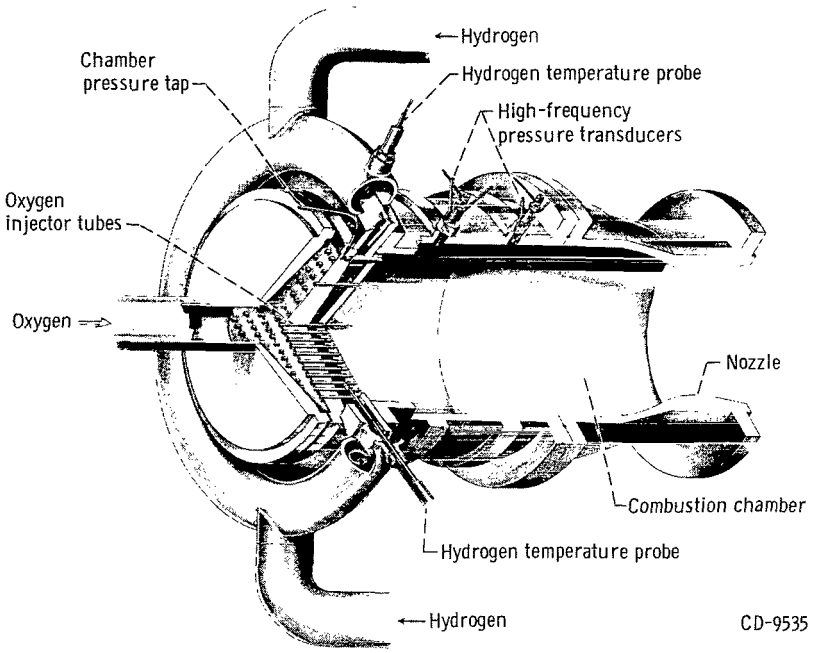

Figure 2. - Sketch of engine.

Injectors

The injectors used in this investigation were of the concentric tube type with each element consisting of a central oxidizer tube surrounded by a concentric hydrogen annulus. Injector faceplate views and element sections are presented in figure 3. The number of elements, dimensions and other details of the injectors are listed in table I. As noted in the table, the injectors had either 1/8-inch (3.175-mm) nickel faceplates or copper faceplates of various thicknesses. The eight-element injector (ref. 4) had interchangeable elements and a stainless-steel transpiration-cooled mesh faceplate as shown in figure 3(g). Except for the eight-element injector, the injector hydrogen-to-oxygen area ratios ranged from 5.03 to 6.11 for the injectors discussed herein. On the basis of the results presented in reference 3, the differences in the area ratios would not have a large effect on the combustion stability and the area ratio magnitudes for the present size engines were large enough so that instability could occur at low hydrogen-injection temperatures.

A geometric parameter of importance to combustion stability is the completeness of faceplate coverage by uniformly spaced injector elements. The present injectors were made with concentric lines of elements such that a uniform increment in injector radius existed between each line. The number of elements per line was such that a uniform area per element was provided. When the outer line of elements was one half the incre-

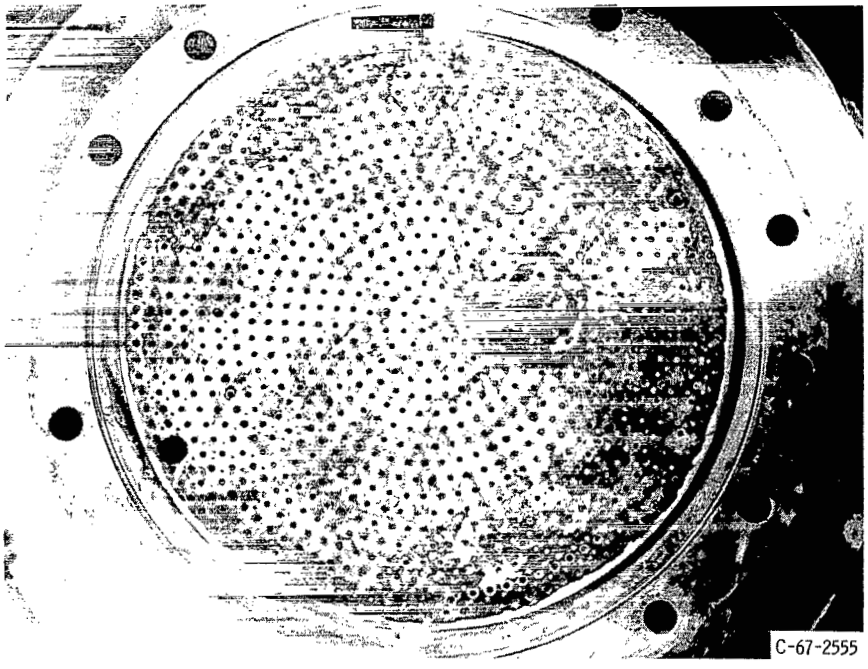

(a) 992 Elements; thrust per element, 20 pounds (89 N).

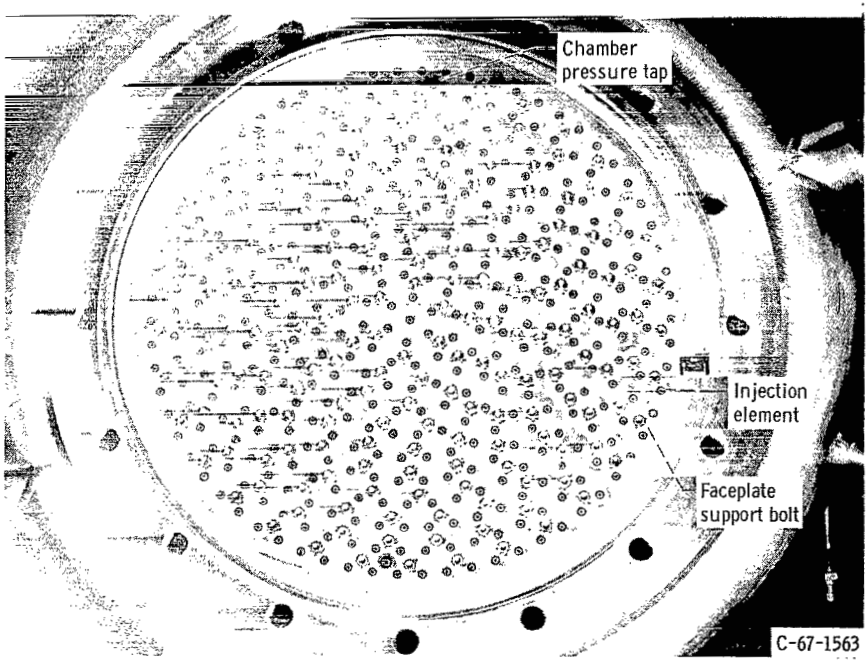

(b) 397 Elements; thrust per element, 50 pounds (222 N).

Figure 3. - Face plate views of coaxial injectors.

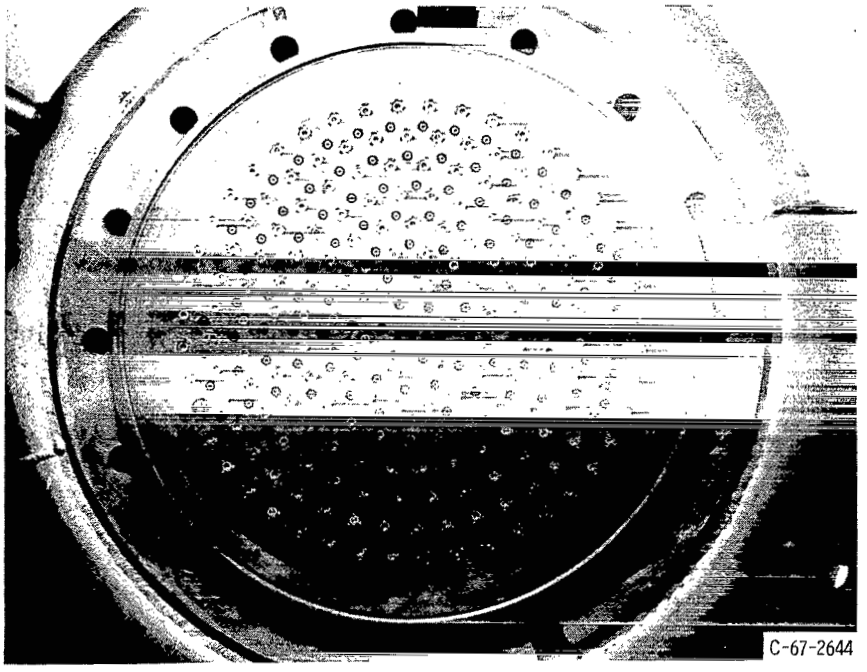

(c) 201 Elements; thrust per element, 100 pounds (445 N).

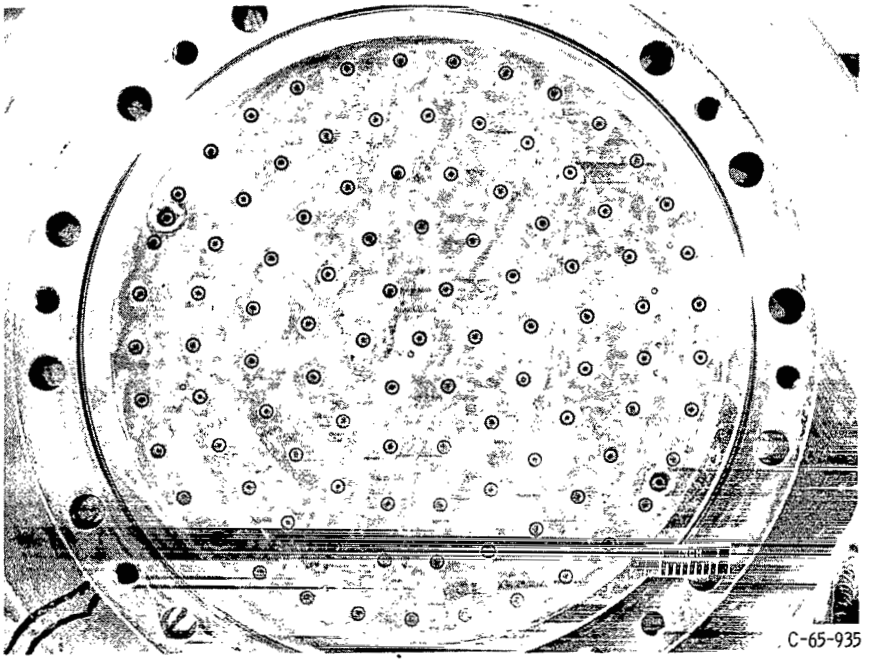

(d) 100 Elements; thrust per element, 200 pounds (890 N).

Figure 3. - Continued.

(e) 35 Elements; thrust per element, 572 pounds (2542 N).

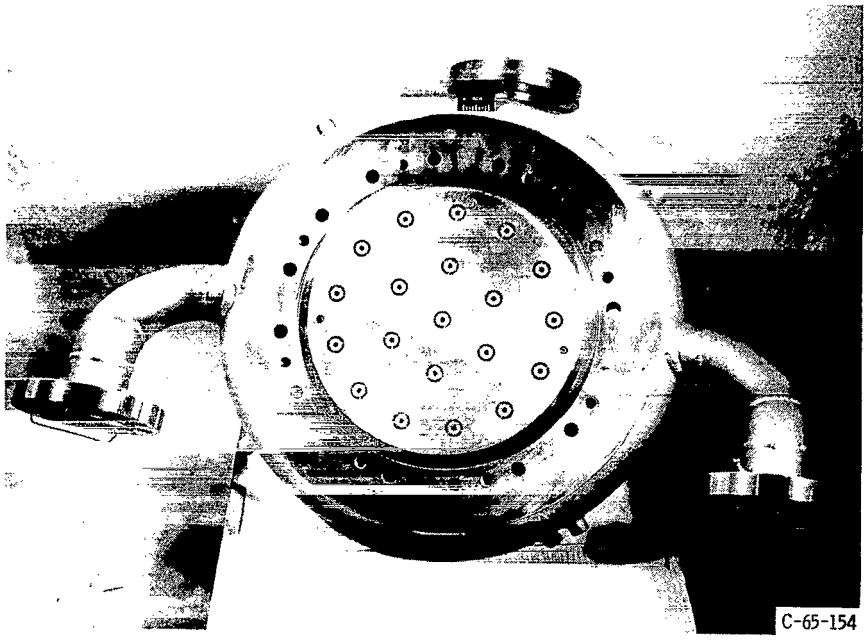

(f) 20 Elements; thrust per element, 1000 pounds (4448 N).

Figure 3. - Continued.

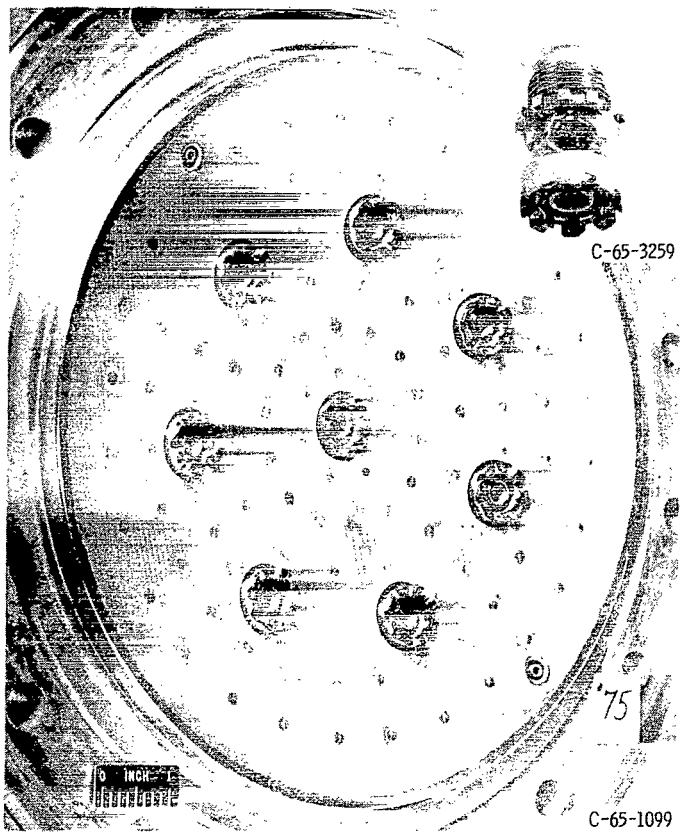

(g) Eight elements; thrust per element, 2500 (11 120 N).

Figure 3. - Concluded.

TABLE I. - INJECTOR DIMENSIONS

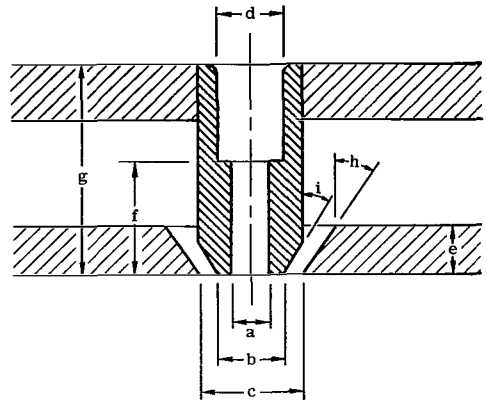

General Element

Number of elements	Thrust per element		Injection area ratio A_{H_2}/A_{O_2}	Oxygen injection area		Hydrogen injection area		Injector	Faceplate percent coverage	Faceplate material
	lb	N		$in.^2$	cm^2	$in.^2$	cm^2			
992	20	88.9	5.6488	0.6328	4.0826	3.5746	23.0619	C2	93.5	Nickel
397	50	222	5.162	.8431	5.4393	4.3525	28.0806	170	100	Copper
201	100	445	6.114	.6068	3.9148	3.710	23.9354	123	100	Copper
100	200	890	5.035	.615	3.9677	3.643	23.5032	C1	100	Copper
32	572	2 544	6.002	.6062	3.9109	3.6383	23.4729	C21	97	Nickel
20	1000	4 448	6.063	.6004	3.8735	3.6402	23.4851	C3	100	Nickel
8	2500	11 120	1.608	1.245	8.0322	2.002	12.9161	75	62	Stainless steel mesh

Number of elements	Injector dimensions[a]																	
	a		b		c		d		e		f		g		h, deg		i, deg	
	in.	cm	in.	cm	in.	cm	in.	cm	in.	cm	in.	cm	in.	cm				
992	0.0285	0.0724	0.0585	0.1486	0.0895	0.2273	0.0625	0.1588	0.125	0.3175	0.30	0.7620	2.94	7.4676	15	0.2618	15	0.2618
397	.052	.1321	.125	.3175	.172	.4369	.109	.2769	.500	1.2700	.410	1.0414	2.41	6.1214	10	.1745	10	.1745
201	.062	.1575	.1300	.3302	.210	.5334	.125	.3175	.750	1.9050	.500	1.2700	2.75	6.9850	15	.2618	15	.2618
100	.0885	.2248	.1595	.4051	.286	.7264	.281	.7137	.125	.3175	.500	1.2700	2.94	7.4676	15	.2618	15	.2618
35	.1485	.3772	.3245	.8242	.4875	1.2383	.500	1.2700	.125	.3175	1.00	2.5400	2.94	7.4676	15	.2618	15	.2618
20	.1955	.4966	.4845	1.2306	.683	1.7348	.625	1.5875	.125	.3175	1.20	3.0480	2.94	7.4676	15	.2618	15	.2618
8	------	------	------	------	------	------	1.123	2.8524	-----	------	-----	------	----	------	15	.2618	0	0

[a]See sketch.

mental radius from the combustion chamber wall, the faceplate coverage was defined as 100 percent. Percent coverage is defined as the square of the ratio of the 100 percent coverage radius to the actual combustion chamber radius multiplied by 100. The injectors used in the present investigation were all within 6.5 percent of 100 percent coverage as indicated by table I.

Bomb Ring

In addition to the usual technique of ramping the hydrogen-injection temperature, attempts to induce combustion instability by the bombing technique were made using a tangential injection bomb ring (fig. 4). The bomb ring, which is described in detail in ref-

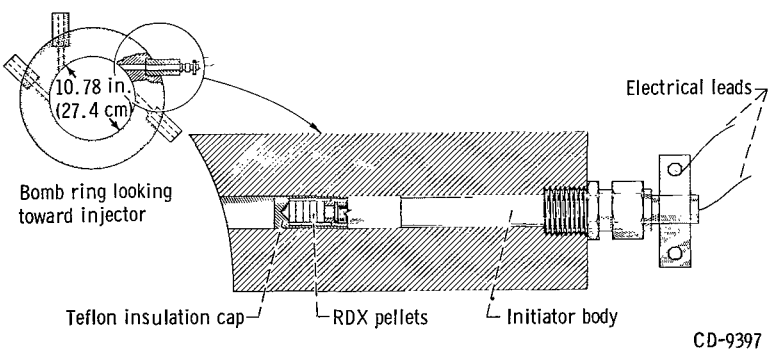

Figure 4. - Details of tangential bomb ring.

erence 5 was made of mild steel and coated on the inside with zirconium oxide. It was located between the injector and the cylindrical combustion chamber and added $3\frac{1}{4}$ inches (0.0825 m) to the chamber length. The bomb ring used four 45.23-grain (2.93-g) charges of RDX explosive (MIL-R-398), which were fired sequentially.

Hydrogen Temperature Controller

The hydrogen temperature ramp used to determine the screech limits was accomplished by varying the amount of 60° R liquid hydrogen and ambient temperature gaseous hydrogen in the mixing tube while maintaining a constant flow rate. Mixing was accomplished by swirling the liquid into the gaseous hydrogen stream. The mixing section was 4 feet (1.312 m) long and was located just upstream of the injector. The constant oxidant-fuel ratio was maintained by an automatic controller. Three set-point inputs

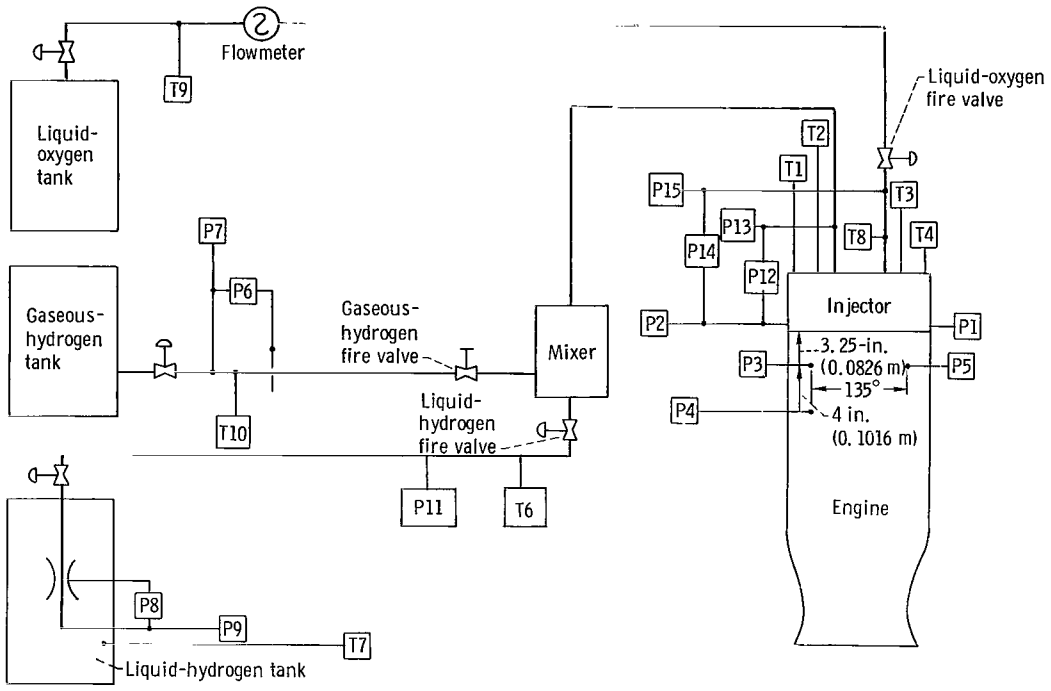

P1 Static chamber pressure (injector face), four-arm strain-gage transducer 1

P2 Static chamber pressure (injector face), four-arm strain-gage transducer 2

P3 Dynamic chamber pressure, water-cooled quartz pressure transducer 3

P4 Dynamic chamber pressure, water-cooled quartz pressure transducer 4

P5 Dynamic chamber pressure, water-cooled quartz pressure transducer 5

P6 Gaseous-hydrogen orifice differential pressure, four-arm strain-gage transducer

P7 Gaseous-hydrogen orifice pressure, four-arm strain-gage transducer

P8 Liquid-hydrogen venturi differential pressure, four-arm strain-gage transducer

P9 Liquid-hydrogen venturi pressure, four-arm strain-gage transducer

P10 Hydrogen-mixer pressure, four-arm strain-gage transducer

P11 Liquid-hydrogen line pressure, four-arm strain gage transducer

P12 Hydrogen-injection differential pressure, four-arm strain-gage transducer

P13 Hydrogen-injection pressure, four-arm strain-gage transducer

P14 Oxygen-injection differential pressure, four-arm strain-gage transducer

P15 Oxygen-injection pressure, four-arm strain-gage transducer

T1 Hydrogen-injector temperature, carbon resistor sensor probe 1

T2 Hydrogen-injector temperature, carbon resistor sensor probe 2

T3 Hydrogen-injector temperature, carbon resistor sensor probe 3

T4 Hydrogen-injector temperature, carbon resistor sensor probe 4

T5 Hydrogen-mixer temperature, carbon resistor sensor probe

T6 Liquid-hydrogen line temperature, carbon resistor sensor probe

T7 Liquid-hydrogen venturi temperature, platinum resistance thermometer

T8 Oxygen-injection temperature, copper-constantan thermocouple

T9 Oxygen flowmeter temperature, platinum resistance thermometer

T10 Gaseous-hydrogen orifice temperature, iron-constantan thermocouple

Figure 5. - Instrumentation diagram.

were required for the automatic controller-chamber pressure, oxidant-fuel ratio, and temperature ramp rate. The oxidizer flow rate was controlled by a closed-loop system which sensed the chamber pressure. The liquid-hydrogen and gaseous-hydrogen flow rates were summed and the total was controlled by adjusting the liquid-hydrogen flow rate to satisfy the oxidant-fuel ratio. The gaseous hydrogen flow rate was controlled by a closed-loop system that sensed the temperature ramp rate selection.

Instrumentation

Location of the various transducers and the associated plumbing are shown by the schematic diagram of figure 5. Except for the high-frequency response types, the transducer signals were transmitted to an automatic digital data recording system. To allow identification of the screech mode, piezoelectric, water-cooled, flushmounted pressure transducers were used. The amplitude response characteristics of the transducers as installed are flat to within 10 percent to a frequency of 6000 hertz and have a nominal resonant frequency of 130 000 hertz. The high-frequency signals were recorded on magnetic tape in analog form and were also displayed on direct reading instruments in the control room for visual monitoring during the tests.

The liquid-oxygen flow rate was determined with a calibrated turbine type flowmeter. The liquid-hydrogen flow rate was measured using a venturi submerged in the supply tank and the gaseous-hydrogen flow rate was measured using an orifice plate. The liquid-propellant temperatures were measured with platinum resistance sensors described in reference 6. The hydrogen-injection temperature was measured using four carbon resistance probes (ref. 7) and were installed as shown in figure 2. The pressure and temperature systems were calibrated immediately prior to data acquisition by an electrical two-step calibration system which used resistances in an electrical circuit to simulate given conditions.

PROCEDURE

In reference 3 it was established that decreasing the hydrogen-injection temperature could lead to unstable combustion in hydrogen-oxygen rocket engines and that the hydrogen temperature at which instability occurred was a good indicator of the sensitivity of the engine to screech. The hydrogen temperature at which combustion instability occurred, called the transition temperature, is therefore a convenient parameter for determining the relative stability of various engine configurations and was used in the present investigation. Hence, lower transition temperatures indicate increased stability and a

temperature ramping technique was employed to determine the transition temperature.

Temperature ramping rates up to 50° R per second (27.76 K/sec) were possible with only small variations in the oxidant-fuel ratio. If by the initial ramping technique the configuration was stable to the minimum hydrogen temperature available with the facility, subsequent runs were made using only the liquid hydrogen.

The combustion performance was determined for a range of hydrogen-injection temperatures by making several runs at essentially constant temperature and analyzing the data obtained at the end of the steady-state period just prior to shutdown.

Engine ignition was accomplished after hydrogen flow was established by injecting a small amount of fluorine into the oxidizer line immediately upstream of the injector simultaneously with actuation of the oxidizer engine valve. Tests were conducted over an oxidant-fuel ratio range of 4 to 6.

The value of the oxidant-fuel ratio at the injector face varied slightly from the controller set value during the hydrogen-temperature ramp. The oxidant-fuel ratio controller responded to signals from the gaseous and liquid-hydrogen flowmeters and the oxygen flowmeter. However, the hydrogen flowmeters were located upstream of the hydrogen mixing tube and as the hydrogen temperature in the mixing tube was decreased by increasing the ratio of liquid to gaseous hydrogen, the effect was also to increase the mass of the hydrogen in the mixing tube. Hence, the amount of hydrogen flowing through the injector was less than the amount indicated by the flowmeters, and the actual oxidant-fuel ratios were slightly higher than the measured values.

Although the facility was equipped with a thrust measuring system, the measurements obtained were not considered sufficiently accurate to present. The characteristic exhaust velocity based on the chamber pressure was used to compare the performance of the various injectors. The chamber pressure was corrected for the momentum pressure loss by the method of Huff, et al., in reference 8. The characteristic exhaust velocity efficiency was based on the theoretical value for equilibrium expansion obtained from the calculations of Gordon and McBride in reference 9. Engine performance data are considered to be accurate to within ±2 percent.

RESULTS AND DISCUSSION

The data pertaining to combustion stability are presented in figures 6 to 11 and will be discussed first, followed by a discussion of combustion efficiency data presented in figures 12 and 13. In addition to the graphical results, a listing of pertinent data for each run is presented as tables II and III.

In the following discussion, thrust-per-element T/E is used as a more descriptive term for element size. It is equivalent to the more fundamental quantity, propellant

TABLE II. - STABILITY DATA

Number of elements, E	Hydrogen-injection temperature, T		Oxidant to fuel ratio, O/F	Chamber pressure at injector, P_c		Total propellant weight flow, $\dot{\omega}_p$		Hydrogen-injector pressure drop, ΔP_h		Oxygen injector pressure drop, ΔP_0		Hydrogen injector velocity, V_h		Injection velocity ratio, V_h/V_0	Characteristic velocity efficiency, η_c, percent	Remarks
	°R	K		psia	N/m^2	lb/sec	kg/sec	psi	N/m^2	psi	N/m^2	ft/sec	m/sec			
992	124	68.9	5.138	310	2137×10^3	59.97	27.20	45	311×10^3	354	2441×10^3	735	224	4.93	100.6	Stable
	78	43.3	5.25	292	2013	61.08	27.71	15	103	381	2627	378	115	2.44	[a]92.7	Transition
	101	56.1	4.069	312	2151	59.42	26.95	42	289	358	2468	645	197	4.46	98.9	
	80	44.1	5.72	294	2027	63.00	28.58	14	97	389	2682	383	117	2.36	[a]92.3	
	82	45.6	3.769	308	2123	60.05	27.24	31	214	318	2193	483	147	3.95	95.9	
	98	54.4	4.478	309	2130	60.70	27.53	38	262	335	2309	599	183	3.99	96.8	
	109	60.6	6.52	298	2055	63.17	28.65	27	186	397	2737	563	172	3.40	96.1	
	89	49.4	4.77	306	2109	61.82	28.04	30	207	348	2399	497	152	3.21	94.6	
397	114	63.3	4.86	317	2186×10^3	58.96	26.74	49	338×10^3	136	937×10^3	911	278	12.56	102.3	Stable
	66	36.7	4.84	348	2399	67.22	30.45	15	103	180	1241	825	252	1.15	98.0	Transition
	68	37.8	3.833	326	2248	64.87	29.43	18	124	157	1082	724	221	1.50	93.1	
	65	36.1	5.67	337	2323	68.35	31.00	11	76	191	1317	678	207	.79	96.3	
	64	35.6	6.15	336	2317	71.46	32.41	10	69	217	1496	711	217	.89	(b)	
201	60	33.3	3.72	319	2199×10^3	58.60	26.58	15	103×10^3	324	2234×10^3	151	46	1.00	97.2	Stable
	62	34.4	4.27	316	2178	61.17	27.75	10	69	336	2317	147	45	.95	96.4	Stable
	62	34.4	4.69	316	2178	59.67	27.07	9	62	329	2268	132	40	.85	99.8	Transition
	64	35.6	5.06	313	2158	62.12	28.18	9	62	370	2551	151	46	.92	96.3	Stable
	63	35.0	4.99	312	2151	62.40	28.30	9	62	371	2558	140	43	.86	94.9	
	65	36.1	5.46	312	2151	65.67	29.79	7	48	425	2930	159	48	.91	91.9	
	60	33.3	3.65	315	2171	60.48	27.43	11	76	299	2062	154	47	1.03	96.2	
100	59	32.8	4.23	288	1985×10^3	56.03	25.42	8	55×10^3	265	1827×10^3	130	40	0.74	96.6	Stable
	57	31.7	5.88	311	2144	67.48	30.61	8	55	423	2916	115	35	.58	92.6	Stable
35	77	42.8	5.24	198	1365×10^3	54.72	24.82	30	207×10^3	541	3730×10^3	533	163	3.55	70.3	Stable
	65	36.1	5.03	245	1689	62.21	28.22	17	117	505	3482	273	83	1.62	75.7	
	68	37.8	5.07	301	2075	62.45	28.33	12	83	405	2792	223	68	1.32	92.5	
	58	32.2	5.27	294	2027	62.62	28.40	6	41	416	2868	121	37	.71	90.4	
20	55	30.6	4.89	222	1531×10^3	66.27	30.06	12	83×10^3	367	2530×10^3	123	38	0.69	63.9	Stable
	56	31.1	6.07	215	1482	66.58	30.20	11	76	397	2737	105	32	.58	64.4	Stable

[a]Injector hydrogen weight flow less than indicated value because of mixing-tube storage. See PROCEDURE section.

[b]Performance data not computed due to nozzle throat erosion.

TABLE III. - PERFORMANCE DATA

Number of elements, E	Hydrogen-injection temperature, T		Oxidant to fuel ratio, O/F	Characteristic velocity efficiency, ηc^*, percent	Number of elements, E	Hydrogen injection temperature, T		Oxidant to fuel ratio, O/F	Characteristic velocity efficiency, ηc^*, percent
	^oR	K				^oR	K		
992	102	56.7	4.02	99.0	100	90	50.0	4.47	95.7
	122	67.8	3.88	99.4		105	58.3	5.90	98.1
	161	89.4	4.71	99.8		106	58.9	4.60	95.5
	194	107.8	4.96	100.4	35	56	31.1	4.43	77.2
397	114	63.3	5.02	97.8		65	36.1	4.98	75.7
	125	69.4	4.97	98.2		144	80.0	4.58	82.9
	136	75.6	5.11	98.5		168	93.3	4.89	84.3
	146	82.8	4.42	98.8		206	114.4	5.71	89.4
201	60	33.3	4.16	96.5	20	55	30.6	4.85	64.3
	63	35.0	5.16	95.2		56	31.1	6.08	64.5
	65	36.1	5.07	96.4		88	48.9	5.28	72.8
						169	93.9	5.16	85.3
100	58	32.2	4.06	96.5		229	127.2	5.32	90.7
	58	32.2	5.96	94.5					
	89	49.4	6.05	97.5					

weight-flow per element. The T/E is based on the thrust obtained with the engine operating at sea level with a 1.3 area ratio exhaust nozzle. The propellant weight flow is listed in table II for each data point.

Combustion Stability

Effect of thrust-per element. - The hydrogen-injection temperature at which combustion instability occurred for each of the injectors is presented in figure 6 as a function of thrust-per-element for a constant oxidant-fuel ratio of 5 (obtained by crossplotting the data of fig. 8). For the stable injectors, the minimum hydrogen temperature tested is shown. The results of figure 6 show a very strong stabilizing influence of increasing T/E. No instability was obtained for injectors having a T/E of 200 pounds (889.6 N) or more. Of several test runs with the 100-pound (444.8 N) T/E injector, only one transition point was obtained at about the minimum hydrogen-injection temperature attainable in the facility.

To further evaluate the stability of the high T/E injectors, a bomb rating technique was employed. The 572-pound (2542-N) T/E and 1000-pound (4448-N) T/E injectors

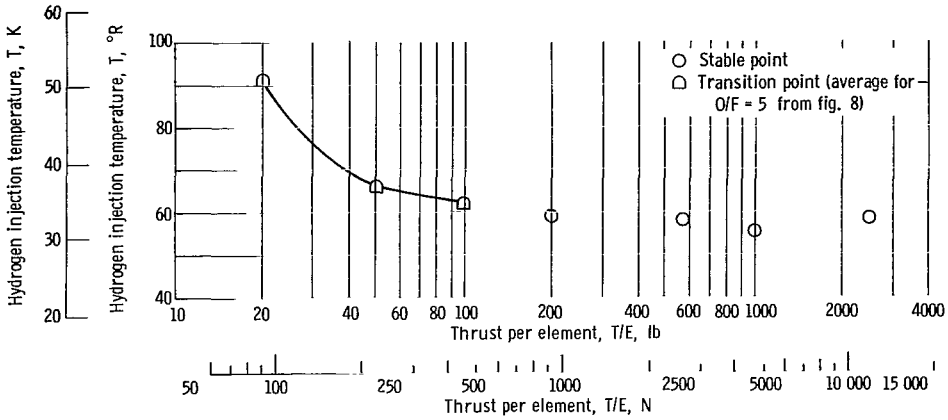

Figure 6. - Effect of thrust per element on minimum hydrogen temperature for stable combustion.

were bombed with four successive 45.23-grain (2.93-g) charges of RDX (MIL-R-398) using a tangential bomb ring between the injector and the cylindrical combustion chamber. In each case, the resulting perturbations were damped out in less than 20 milliseconds as shown by the high-frequency pressure traces presented in figure 7. The bomb pressure spikes were over 300 psi (2.068 MN/m^2) above the steady-state chamber pressure of 300 psia (2.068 MN/m^2).

Although it is clear that the high T/E injectors were extremely stable for the engine size tested, experience has shown that combustion stability deteriorates when rocket en-

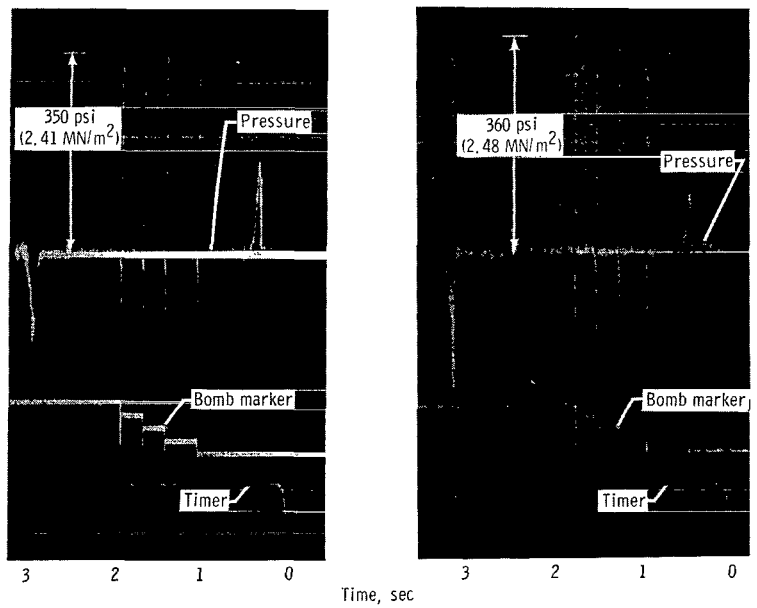

(a) 35 Elements; thrust per element, 572 pounds (2542 N).

(b) 20 Elements; thrust per element, 1000 pounds (4448 N).

Figure 7. - Pressure traces of bomb tests.

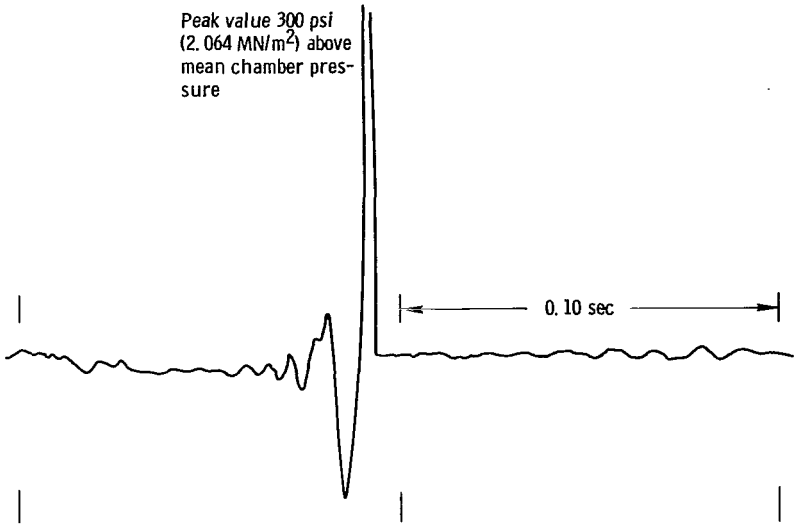

(c) Expanded trace of bomb spike for 35-element, 572-pound (2542-N) thrust-per-element injector.

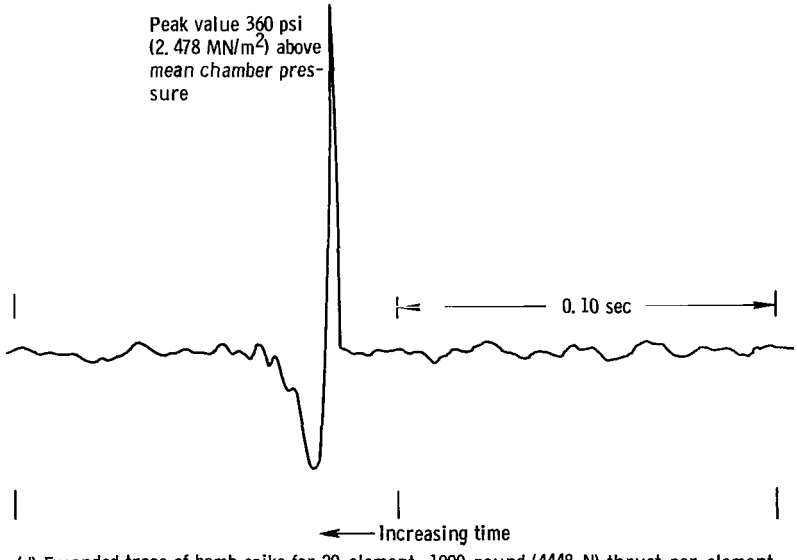

(d) Expanded trace of bomb spike for 20-element, 1000-pound (4448-N) thrust-per-element injector.

Figure 7. - Concluded.

gines are scaled up in size. For example, the M-1 rocket engine, which has a combustion chamber diameter of 42 inches (1.066 m) and an injector with a T/E of 462 pounds (2070 N), was unstable at hydrogen-injection temperatures below 79° R (43.9 K) (ref. 10); whereas, the same injector elements in a 5.39-inch (0.136-m) diameter engine were completely stable (ref. 11). It is expected, however, that the trend to increased stability for increasing T/E would be true for large engines also and that the variation in the hydrogen-transition temperature with T/E as shown by the curve of figure 6 is typical of a family of such curves where similar curves for larger engines would be displaced to a higher T/E range.

Correlating parameters. - It was shown in reference 3 that the hydrogen-to-oxygen velocity ratio at the injector face defined a screech boundary for a series of constant T/E injectors. The constant velocity ratio parameter correlated the effects of varying the O/F and the propellant-injection area ratio. The expression for the velocity ratio

$$\left(\frac{V_h}{V_o}\right) = \left(\frac{A_o}{A_h}\right)\left(\frac{\rho_o}{\rho_h}\right)\left(\frac{1}{O/F}\right)$$

shows that it is a function of the oxidant to fuel propellant area ratio A_o/A_h, the oxidant-fuel ratio, O/F, and the oxidant to fuel propellant density ratio ρ_o/ρ_h. For a given injector, the area ratio is a constant. The liquid-oxygen temperature and hence density are not significantly affected by the variations in the hydrogen temperature during the ramping technique. Therefore, as the O/F is increased, a constant velocity ratio requires a decrease in the hydrogen density which corresponds to an increase in the hydrogen temperature.

The experimental transition hydrogen temperatures for the T/E of 20-, 50-, and 100-pound (89-, 222-, and 445-N) injectors (only configurations for which a stability limit could be defined) are presented as functions of the oxidant-fuel ratio in figure 8. Although the data showed a considerable amount of scatter, the stability limit for each configuration was in general agreement with a line of constant velocity ratio. However, the magnitude of the velocity ratio parameter at transition differed for each injector and decreased as the T/E was increased.

The general agreement of the experimental data with the constant-velocity-ratio lines prompted the search for an improved correlating factor to account for the effects of T/E. Such a correlation is presented in figure 9(a). Weighted-velocity ratios for each data point were obtained by multiplying the velocity ratio by the propellant weight flow per element. A transition zone at a value of the parameter of about 0.2 is defined for all three injectors.

Concurrently with the development of the weighted-velocity-ratio parameter, another empirical correlating factor W_{cr} (ref. 12) was derived from experiments in which weight

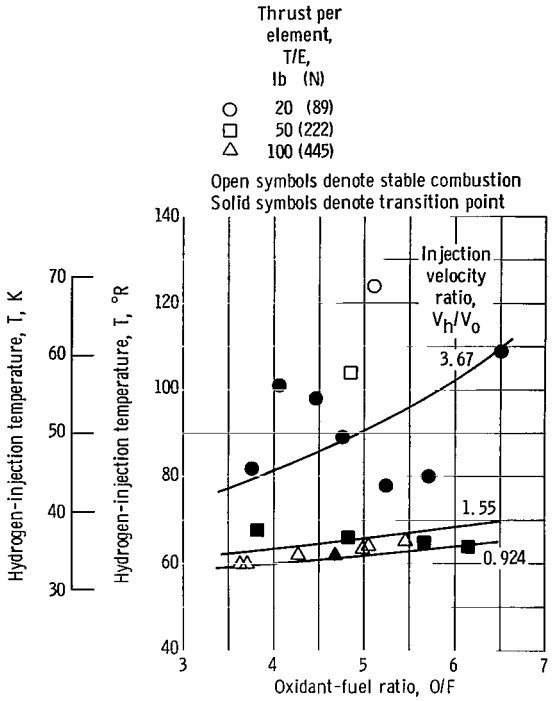

Figure 8. - Hydrogen-transition temperature variation with oxidant-fuel ratio.

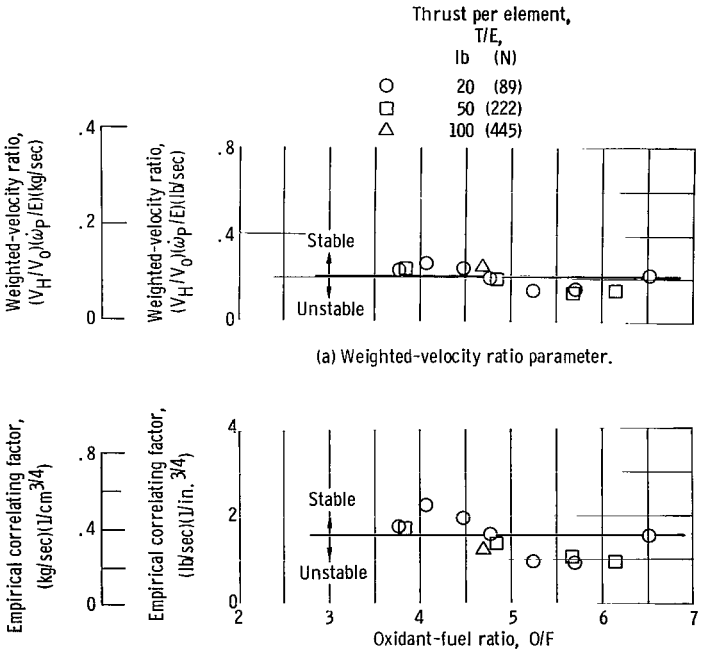

(a) Weighted-velocity ratio parameter.

(b) W_{cr} parameter of reference 12.

Figure 9. - Correlation of transition point data with weighted-velocity ratio parameter and with W_{cr}.

flow, chamber pressure, and nozzle throat area were varied. The factor W_{cr} is defined by the equation:

$$W_{cr} = \sqrt{\frac{2g\,\Delta P_h}{\rho_h}}\,\rho_o D_o^{1.25}\sqrt{\frac{1}{O/F}} \tag{2}$$

where ΔP_h is the hydrogen-injector pressure drop and D_o is the oxygen tube exit diameter. A correlation of the present data using equation (2) is shown in figure 9(b). As can be seen, the stability limit was defined equally well by both parameters. Equation (2) indicates that the stability effects of changing the element size or thrust per element are primarily associated with changes in D_o, and thus with oxygen ligimentation or droplet size.

The deviations of the experimental data from the constant mean value of the correlating parameters may result from two factors, experimental error and/or some small variations in element design. For example, referring to table I for the unstable injectors, faceplate thickness ranged from 0.125 to 0.210 inch (0.317 to 0.533 cm), injector angle from 10^o to 15^o, and injection area ratio from 5.162 to 6.114. Considering the relatively good agreement of the data with correlating parameters that do not have provisions for equating these design variations to stability, it can be concluded that the range of variations of these geometric parameters in the present tests had a small influence on the stability limit. Other geometric variables such as the oxygen tube recess and nonuniform element coverage of the face-plate area have been shown to have large effects on the combustion stability. It is believed that this effect, that is, the strong destabilizing effect of leaving an annular area at the periphery of the injector face void of injector elements (as shown in ref. 13), was the reason that the magnitude of the W_{cr} parameter obtained in the present tests differed from that determined in reference 12.

Figure 10 presents the weighted-velocity ratios at the minimum hydrogen temperature for the stable high T/E injectors relative to the transition zone. The increase in stability with increasing T/E is again indicated by the increase in the distance of the points above the transition line with increasing T/E. The weighted-velocity ratio of 7.5 for the T/E = 2500 injector was too large to show on the graph of figure 9.

In reference 2, it was shown that a high-frequency combustion instability analysis, based on the dynamic response characteristics of the propellant flow system and the engine geometry, showed general agreement with the trends of the experimental results reported in reference 3. The analysis of reference 2 includes the response characteristics of the gaseous-hydrogen flow through the injector, the liquid-oxygen drop vaporization, and the exit nozzle. In the comparison of the analytical results with the data from reference 3, both the oxygen response factor and the exit nozzle response were assumed constant. These assumptions were in agreement with the test conditions of reference 3

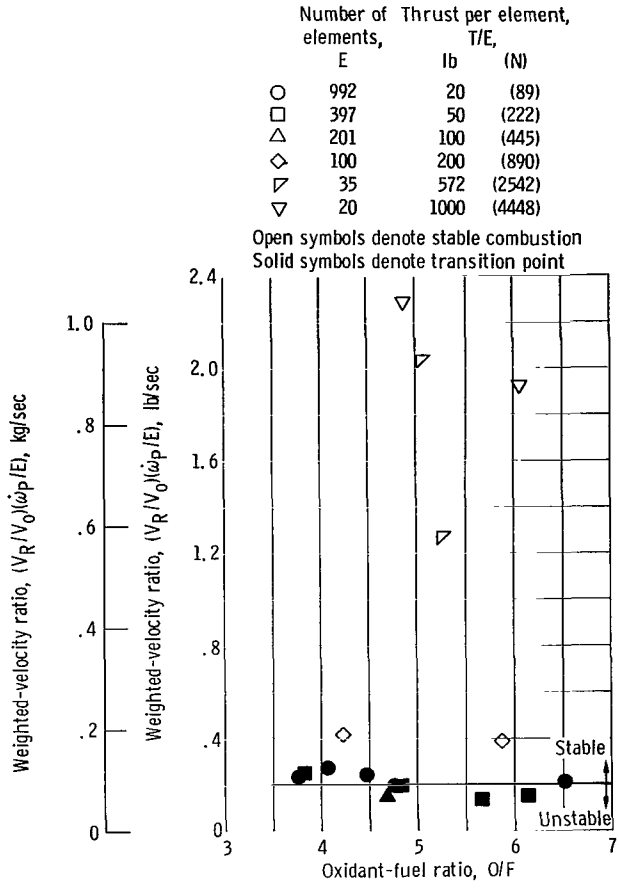

Figure 10. - Variation of weighted-velocity ratio at transition point or at minimum hydrogen temperatures for all injectors.

where the oxygen orifice diameter and the nozzle geometry were not varied. The response model analytical technique has not been developed to the point, however, where quantitative changes in the oxygen response factor can be predicted when the oxygen jet diameter varies. Therefore, no attempt was made to use this analytical technique to correlate the present results.

Instability modes. - The instability frequencies for those injectors having transition points are shown in figure 11. The stabilizing influence of increasing T/E is again evident in the decrease of the combustion instability amplitude with increasing T/E. The lowest thrust-per-element injector exhibited a second harmonic tangential mode of about 5400 hertz with a peak-to-peak amplitude of about 50 percent of the chamber pressure. The T/E = 50 injector exhibited a fundamental tangential mode at approximately 3400 hertz with an amplitude of about 30 percent of the chamber pressure. At a T/E = 100, the first-tangential mode was still predominant, but its amplitude was only 12 per-

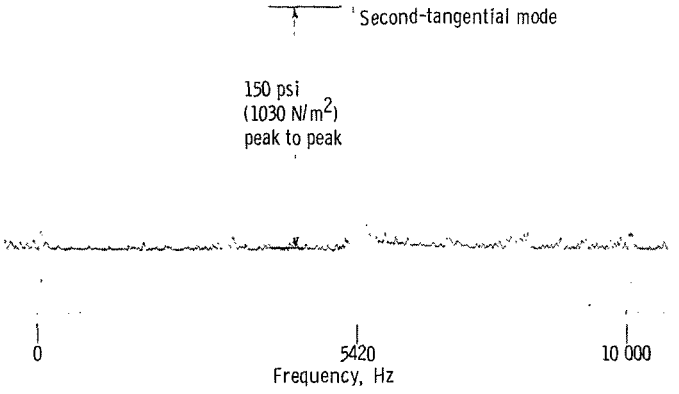

(a) 992 Elements; thrust per element, 20 pounds (89 N); oxidant-fuel ratio, 5.27.

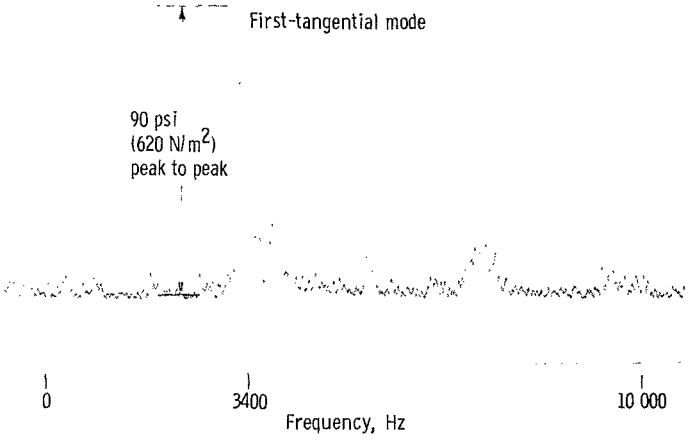

(b) 397 Elements; thrust per element, 50 pounds (222 N); oxidant-fuel ratio, 4.84.

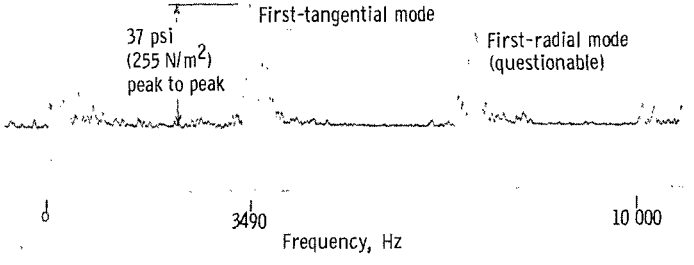

(c) 201 Elements; thrust per element, 100 pounds (445 N); oxidant-fuel ratio, 4.69.

Figure 11. - Typical amplitude spectral density graphs for coaxial injectors.

cent peak-to-peak of the chamber pressure of 300 psia (2.064 MN/m^2). However, the oscillations at about 7150 hertz for the T/E = 100 injector, though not exactly identifiable, are close to those representing the first-radial mode. At T/E values of 200 and above, no screech was encountered.

Combustion Performance

Rocket-engine design criteria specify that for high-combustion efficiency the injector should produce fine atomization and uniform mixing of the propellants. This is generally obtained by using injectors with many fine elements. It has been shown, however, that the use of large T/E injectors (i.e., a few large injector elements) is beneficial to combustion stability. It appears, therefore, that the injector design criteria for combustion stability are contrary to those for combustion efficiency and that the gains in combustion stability by increasing T/E would be obtained at the expense of combustion performance.

The combustion performance, as indicated by the characteristic velocity efficiency ηC^*, is presented in figures 12 and 13 as functions of the T/E and the hydrogen-injection temperature, respectively. Figure 12 shows that at a hydrogen-injection temperature of 150° R (84.5 K) ηC^* decreased gradually with increasing T/E from a value of 99.5 percent at T/E equal 20 pounds (88.9 N) to 97.5 percent at a T/E of 200 pounds (88.64 N). At T/E values greater than 200 pounds (889.64 N), ηC^* decreased very rapidly with increasing T/E. A similar variation in ηC^* with T/E was shown by the lower ηC^*

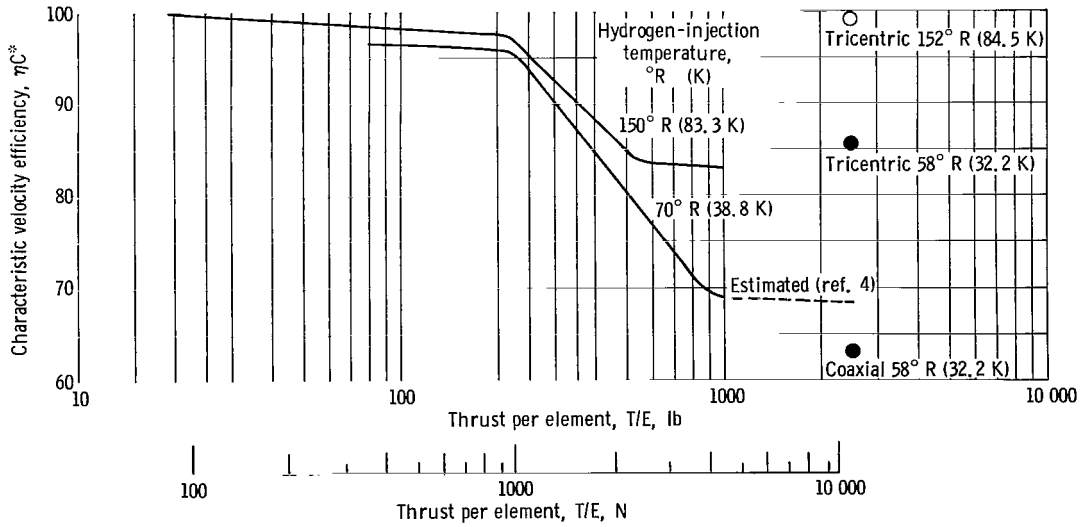

Figure 12. - Effect of thrust per element on the characteristic exhaust velocity efficiency at hydrogen-inlet temperatures of 150° and 70° R (83.3 and 38.8 K). Data points from reference 4.

values at a hydrogen-injection temperature of 70° R (38.9 K). The trade-off in performance to gain stable combustion at all hydrogen-injection temperatures was equal to a 2 percent decrease in the ηC^* for the present case because complete stability was obtained a T/E of 200 pounds (889.64 N).

The combustion efficiency also decreased with decreasing hydrogen-injection temperature (fig. 13). The poorest combustion performance would therefore be obtained with engines having large T/E injectors and low hydrogen-injection temperatures. Hence, the optimum element size with regard to both stability and performance depends on the hydrogen-injection temperature. The hydrogen-injection temperature varies with the size and type of engine. For example, in a small regeneratively cooled engine, the hydrogen temperature will be high (300° R (166.6 K) for RL-10), which allows the use of fine elements for maximum performance without screech. In a large engine, as the M-1, the hydrogen-injection temperature will be about 140° R (77.8 K) because a smaller coolant load per pound (Kg) of hydrogen exists. Larger elements for a higher T/E will be required, but the efficiency can still be high. In a large ablatively cooled engine however, the hydrogen-injection temperatures will be in the 50° to 60° R (27.8 to 33.3 K) range,

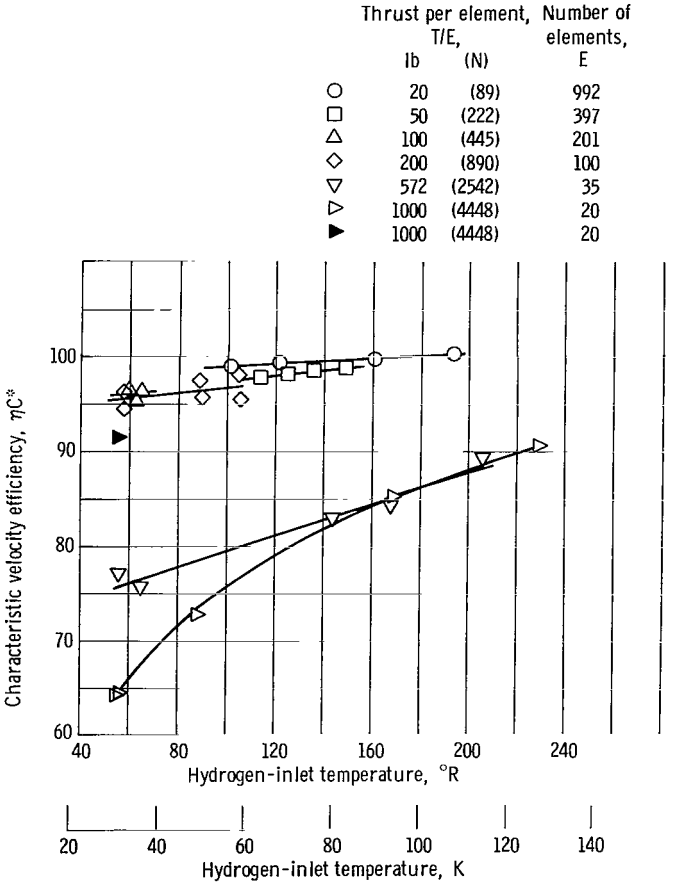

Figure 13. - Effect of hydrogen temperature on combustion efficiency as indicated by characteristic velocity efficiency. Combustion chamber length, 12 inches (0.305 m) except for solid symbol where length equals 22 inches (0.559 m).

which penalizes performance particularly for large T/E injectors that would be required for stability. This case poses a challenging problem to engine designers to improve the combustion performance of high T/E injectors.

That large improvements in combustion stability can be made for high T/E injectors has been demonstrated. Reference 4 reports the results of an injector-element improvement program for the eight-element 2500-pound (11 120-N) T/E injector. For a simple coaxial injector element, such as those for the injectors of the present program, a ηC^* of only 63 percent was obtained at a hydrogen-injection temperature of 58° R (32.2 K). This low efficiency was increased to 85.5 percent by the use of a tricentric element. It is interesting to note also that at a higher hydrogen temperature (152° R (84.5 K)) the best element configuration tested in reference 4 (as shown in table I) had a ηC^* of 99 percent. The data points mentioned for the 2500-pound (11 120-N) T/E injector are shown on the C* performance chart of figure 12.

Other methods of increasing the combustion efficiency, such as optimizing the combustor length can also be employed. For example, increasing the combustion chamber length from 12 to 22 inches (0.305 to 0.559 m) for the 1000-pound (4448-N) T/E injector raised ηC^* at 55° R (30.5 K) from 64.5 percent to 91.5 percent (fig. 13). It should not be construed, however, that 100-percent efficiency can be obtained by increasing the combustion chamber length only.

CONCLUDING REMARKS

An experimental investigation of the effects of thrust per element with 10.78-inch (0.274-m) coaxial injectors on a 20 000-pound (99 964-N) thrust oxygen-hydrogen rocket engine indicated that

1. Increasing the injector thrust per element in the range from 20 to 100 pounds (88.96 to 444.92 N) increases the combustion stability as indicated by the lower hydrogen-injection temperatures required to induce unstable combustion. At thrust-per-element values of 200 pounds (889.64 N) and above, no instability could be induced even with large bombs and the lowest hydrogen temperatures available at the facility.

2. The stability transition data correlated with both the parameter obtained from multiplying the injection velocity ratio by the weight flow per element and with the W_{cr} parameter of reference 12. However, due to differences in the injection element distribution over the faceplate between the present injectors and those of reference 12, the present data correlated at a different magnitude of the W_{cr} parameter than did the data in reference 12.

3. At high hydrogen-injection temperatures (150° R (83.4 K)) the characteristic velocity efficiency decreased gradually with increasing thrust per element from a value

of 99.5 percent at a thrust per element of 20 pounds (88.96 N) to about 97.5 percent at a thrust per element of 200 pounds (889.64 N). Above a thrust per element of 200 (889.64 N), the characteristic velocity efficiency decreased very rapidly with increasing thrust per element. The trend was similar for lower characteristic velocity efficiencies at a hydrogen-injection temperature of 70° R (38.9 K).

4. For all injectors tested, the characteristic velocity efficiency decreased with decreasing hydrogen-injection temperature.

Lewis Research Center,
National Aeronautics and Space Administration,
Cleveland, Ohio, June 20, 1968,
128-31-06-05-22.

REFERENCES

1. Crocco, Luigi; and Cheng, Sin-I: Theory of Combustion Instability in Liquid Propellant Rocket Motors. Butterworth Scientific Publ., 1956.

2. Feiler, Charles E.; and Heidmann, Marcus F.: Dynamic Response of Gaseous-Hydrogen Flow System and its Application to High-Frequency Combustion Instability. NASA TN D-4040, 1967.

3. Wanhainen, John P.; Parish, Harold C.; and Conrad, E. William: Effect of Propellant Injection Velocity on Screech in 20,000-Pound Hydrogen-Oxygen Rocket Engine. NASA TN D-3373, 1966.

4. Hannum, Ned P.; and Conrad, E. William: Performance and Screech Characteristics of a Series of 2500-Pound Thrust-per-Element Injectors for a Liquid-Oxygen-Hydrogen Rocket Engine. NASA TM X-1253, 1966.

5. Tabata, William K.; Antl, Robert J.; and Vincent, David W.: Storable Propellant Combustion Instability Program at Lewis Research Center. Paper No. 66-602, AIAA, June 1966.

6. Ladd, J. W.: A Durable and Reliable Test Stand System for High-Accuracy Temperature Measurements in the Cryogenic Ranges of Liquid Hydrogen and Liquid Oxygen. Advances in Cryogenic Engineering. Vol. 6. K. D. Timmerhaus, ed., Plenum Press, 1961, pp. 388-395.

7. Herr, Austin C.; Terbeek, Howard G.; and Tiefferman, Marvin W.: Suitability of Carbon Resistors for Field Measurements of Temperatures in the Range of 35° to 100° R. NASA TN D-264, 1960.

8. Huff, Vearl N.; Fortini, Anthony; and Gordon, Sanford: Theoretical Performance of JP-4 Fuel and Liquid Oxygen as a Rocket Propellant. II - Equilibrium Composition. NACA RM E56D23, 1956.

9. Gordon, Sanford; and McBride, Bonnie J.: Theoretical Performance of Liquid Hydrogen with Liquid Oxygen as a Rocket Propellant. NASA Memo 5-21-59E, 1959.

10. Dankoff, Walter F.; Johnsen, Irving A.; Conrad, E. William; and Tomazic, William A.: M-1 Injector Development - Philosophy and Implementation. NASA TN D-4730, 1968.

11. Scott, Herbert E.; Bloomer, Harry E.; and Mansour, Ali H.: M-1 Engine Subscale Injector Tests. NASA TN D-4053, 1967.

12. Wanhainen, John P.; Feiler, Charles E.; and Morgan, C. Joe: Influence of Chamber Pressure, Flow Per Element and Contraction Ratio on Acoustic-Mode Instability in Hydrogen-Oxygen Rockets. NASA TN D-4733, 1968.

13. Bloomer, Harry E.; Wanhainen, John P.; and Vincent, David W.: Chamber Shape Effects on Combustion Instability. Presented at the 4th ICRPB Combustion Conference, Menlo Park, Calif., Oct. 2-13, 1967.

NASA-Langley, 1968 —— 28 E-4511

"The aeronautical and space activities of the United States shall be conducted so as to contribute . . . to the expansion of human knowledge of phenomena in the atmosphere and space. The Administration shall provide for the widest practicable and appropriate dissemination of information concerning its activities and the results thereof."

— NATIONAL AERONAUTICS AND SPACE ACT OF 1958

NASA SCIENTIFIC AND TECHNICAL PUBLICATIONS

TECHNICAL REPORTS: Scientific and technical information considered important, complete, and a lasting contribution to existing knowledge.

TECHNICAL NOTES: Information less broad in scope but nevertheless of importance as a contribution to existing knowledge.

TECHNICAL MEMORANDUMS: Information receiving limited distribution because of preliminary data, security classification, or other reasons.

CONTRACTOR REPORTS: Scientific and technical information generated under a NASA contract or grant and considered an important contribution to existing knowledge.

TECHNICAL TRANSLATIONS: Information published in a foreign language considered to merit NASA distribution in English.

SPECIAL PUBLICATIONS: Information derived from or of value to NASA activities. Publications include conference proceedings, monographs, data compilations, handbooks, sourcebooks, and special bibliographies.

TECHNOLOGY UTILIZATION PUBLICATIONS: Information on technology used by NASA that may be of particular interest in commercial and other non-aerospace applications. Publications include Tech Briefs, Technology Utilization Reports and Notes, and Technology Surveys.

Details on the availability of these publications may be obtained from:

SCIENTIFIC AND TECHNICAL INFORMATION DIVISION

NATIONAL AERONAUTICS AND SPACE ADMINISTRATION

Washington, D.C. 20546